Esterase 2 as a fluorescent biosensor for the detection of organophosphorus compounds: docking and electronic insights from molecular dynamics.

Ingrid G. Prandi[1,2,*]; Teodorico C. Ramalho[1,2]; Tanos C. C. França[2,3]

[1]*Department of Chemistry, Federal University of Lavras, 37200-000, Lavras, Brazil;*

[2]*Laboratory of Molecular Modeling Applied to the Chemical and Biological Defense, Military Institute of Engineering, Praça Gen. Tibúrcio, 80, Rio de Janeiro, Brazil;*

[3]*Faculty of Informatics and Management, Center for Basic and Applied Research, University of Hradec Králové, Rokitanskeho, 62, 50003 – Hradec Králove, Czech Republic*

Abstract

Organophosphorus compounds (OP) are mainly used in agriculture as pesticides. Unfortunately, each year many rural workers die intoxicated by those compounds. Sometimes the diagnosis of the exact molecule that caused the intoxication can be tardy, exposing patients to a huge risk. Esterase 2 from *Alicyclobacillus acidocaldarius* is a potential fluorescent biosensor for OP intoxication and although it has been well studied in an experimental way, the complete understanding of the energy transfer processes that occur between the *Aa*EST2 enzyme and OP ligands (like chlorpyriphos, diazinon, parathion and paraoxon) are still obscure. In this work, we applied computational chemistry methodologies as molecular docking and molecular dynamics and Förster fluorescence resonance energy transfer (FRET) theory to have a better understanding of the fluorescence profiles that are described in the literature.

Keywords:

Esterase 2, chlorpyriphos, diazinon, parathion, paraoxon

*Correspondence author: ingrid.prandi@gmail.com

Introduction

Organophosphorus compounds (OP), are biodegradable molecules characterized as organic compounds containing C-P bounds. OPs are mainly used in agriculture as pesticides in replacement to the non-biodegradable organochlorine pesticides[1], but, due to its toxic effects, some of them have been used as chemical weapons both in regular wars and terrorist attacks[2,3] despite being banned by the Chemical Weapons Convention (CWC)[4] since 1997.

The first step to treat a patient intoxicated by an OP is to specifically identify the harmful compound. In literature, previous studies show that OPs are known as strong competitive inhibitors of the enzyme acetylcholinesterase (AChE)[2,3,5], which catalyses the hydrolysis of the ester group of the neurotransmitter acetycholine (ACh), yielding acetic acid and choline (Ch) as products. This fact has pointed to the possibility of using an esterase as biological sensor for OPs[5,6]. In particular, the esterase EST2 from *Alicyclobacillus acidocaldarius* (*Aa*EST2)[7] has been reported as a potential OPs biosensor, since it has been shown that the presence of this enzyme in an environment containing OPs, can change the fluorescence response when light in the right wavelength falls onto the sample. Indeed, the variation in the fluorescence signal is able to quantitatively identify this compounds in concentrations ranging from nano to picomolars[6].

Many computational and experimental techniques are based on Förster resonance energy transfer (FRET) theory[8]. It is often employed as a powerful tool to determine interactions between protein and ligands by a fluorescence response.[9,10] Tryptophan is

one of the three fluorescent amino acids and it is the greatest natural protein source of UV absorption and emission.[9,11] In this work we investigate the tryptophan fluorescence quenching of *Aa*EST2 described by some literature experimental results[6] with new theoretical calculations: molecular docking, MD dynamics and results from a new method for fluorescence insights based on FRET. The case studies are the OP ligands: chlorpyriphos, diazinon, parathion and paraoxon (Figure 1).

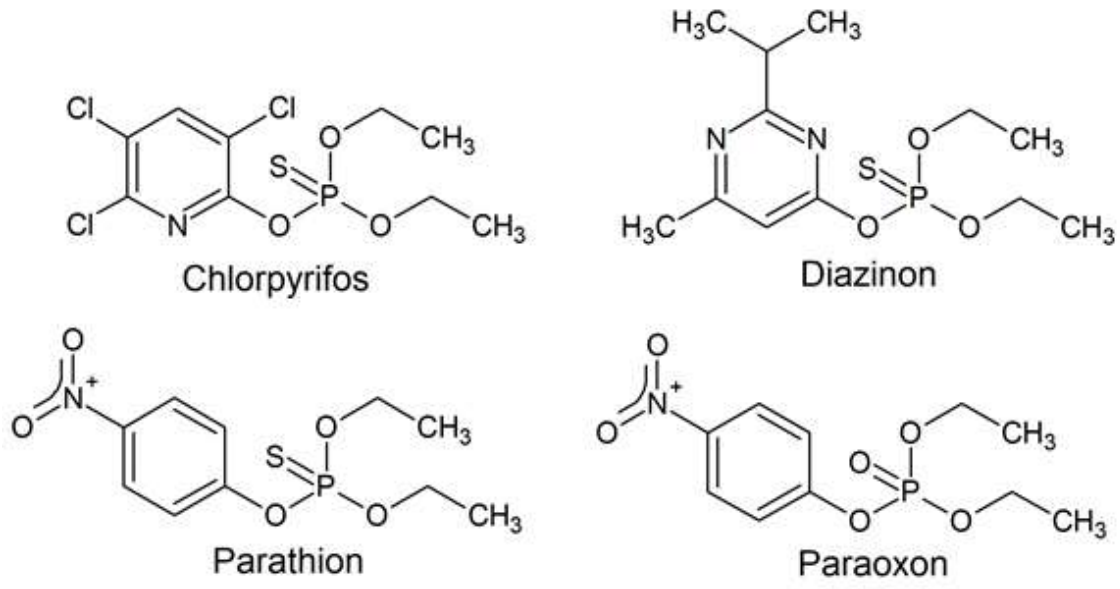

Figure 1: Pesticides able to inhibit EST2 enzyme.

Methodology

In this section, we discuss the computational details and the base theory for a better understanding of this work.

Before starting the docking procedure, the 3D structures of chlorpyriphos, diazinon, paraoxon and parathion were constructed and optimized using the software PC Spartan Pro[12]. The atomic electrostatic charges were computed using a DFT method (B3LYP/6-31G**), since most of semi-empirical methods like AM1 usually underestimate phosphorous charges.

Docking

For the docking studies we considered the crystal structure of *Aα*EST2[7], resolved at 2.6 Å, and complexed with (4-(2-hydroxyethyl)-1-piperazine ethanesulfonic acid) (HEPES), available in the Protein Data Bank (PDB)[13] under the code 1EVQ. The crystallographic water molecules where kept for the molecular modelling studies, and H atoms were inserted to meet the appropriate residues protonation under physiologic pH. All docking procedures were performed with the Molegro Virtual Docking (VMD) software[14].

We considered as the active site the cavity that contained the molecule HEPES binding inside. All the lateral residues of the amino acids inside the cavity were considered flexible on the minimizing procedure of the docking. 400 different geometries were generated for each pesticide inside *Aα*EST2 and considered the ones with the greatest affinity, the highest interactions with the protein and the most promisor geometry orientation to bind the active site.

Fluorescence resonance energy transfer (FRET)

From Förster theory[8], the fluorescence resonance energy transfer (FRET) is a molecular non-radiative process that allows the transference of an exciton from a donor to an acceptor. This process can occur if there is superposition of the donor absorbance spectrum and the acceptor emission spectrum.

The electronic coupling between the involved molecules is given by the sum of two contributions as shown in equation (1):

$$V = V^{Coul} + V^{Short} \qquad (1)$$

where V^{Coul} represents the Coulombic interaction and V^{Short} is the short range contribution. Förster model assumes that the short range interactions are weak, implying in $V \approx V^{Coul}$. This model also assumes that the Coulombic coupling can be approximated as a dipole-dipole interaction between the transition dipole moments of the donor (μ_D) and the acceptor (μ_A) (Equation 2):

$$V^{Coul} \approx V^{DD} = \frac{\kappa}{4\pi\varepsilon_0} \frac{|\vec{\mu}_D||\vec{\mu}_A|}{R^3} \qquad (2)$$

where ε_0 is the vacuum electric permissivity, R is the distance between the center of mass of the molecules involved in the energy transference, and κ is the orientation factor defined according to equation 3:

$$\kappa = \hat{\mu}_D \cdot \hat{\mu}_A - 3(\hat{\mu}_D \cdot \hat{R})(\hat{\mu}_A \cdot \hat{R}) \qquad (3)$$

where $\hat{\mu}_D$ and $\hat{\mu}_A$ are the unitary vectors along the transition dipole moments of the donor and the acceptor.

If we consider φ, θ_D , θ_A respectively the angles between $\hat{\mu}_D$ and $\hat{\mu}_A$, $\hat{\mu}_D$ and $\hat{R}$, $\hat{\mu}_A$ and $\hat{R}$, (see Figure 2 for a better visualization) we can write:

$$\kappa = \cos\varphi - 3\cos\theta_D \cos\theta_A \qquad (4)$$

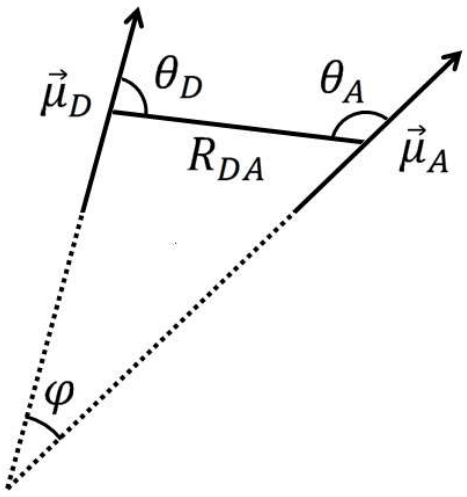

Figure 2: Geometric parameters in Förster theory

For the discussions presented in this work, we considered Förster theory and the energy exchange between the pesticides and the residue Trp85 located in the active site of the *Aa*EST2. Tryptophan residues can present a great fluorescence in protein due to their electronic delocalization of the indole aromatic ring. In the specific case of *Aa*EST2, experimental data point a possible quench of the protein fluorescence: the close proximity of the ligands to the Trp85 ables an energy transfer from the protein residue to the ligand.[6]

Molecular dynamics simulations

The best poses of each pesticide inside *Aa*EST2, selected from the docking studies, were submitted to molecular dynamic simulations with the software GROMACS[15]. The systems *Aa*EST2/OP were solvated inside cubic boxes with the SPC water model[16] and neutralized with 12 Na^+ ions.

The force-field used for the protein description was GROMOS96 43A1[17,18]. On the other hand, for the pesticide we used a set of specific force-fields constructed from their optimized geometry. The parameters were developed by ATB website[19] using the diagonalization of Hessian matrix.

After the preparation step of the simulation boxes, the minimizations of the systems were performed. In this step, we used the steepest descent algorithm with a maximum of 50000 iteration cycles of 10 fs in order to minimize the close contacts. A heating step was performed on the four systems in the NVT ensemble with leap-frog algorithm[20,21]. These 1 ns simulations were done with an integration step of 1 fs. A harmonic potential was used in order to restrain the protein and ligands during the heating procedure. The temperature was controlled by v-rescale thermostat[22] and slowly increased to 300 K. Periodic Boundary Conditions (PBC) were applied and PME (Particle Mesh Ewald)[23] scheme was used for long range interactions.

After the heating process, we performed an equilibrium simulation in the ensemble NPT in order to stabilise the simulation box volume. Yet, with the restrain of the harmonic

potentials, the simulation was performed for 100 ps. The temperature and pressure were respectively controlled by the v-rescale thermostat (300 K) and Parrinello-Rahman barostat (1 bar). As in the heating step we applied the PBC and the PME schemes.

The last simulation step was the performance of 70 ns of MD simulation, in a NPT ensemble, without the constrain potentials. The H-bonds were constrained by the lincs algorithm[24] and the simulation step was increased to 2 fs. The integration algorithm was leap-frog. The thermostat and barostat used were v-rescale (300 K) and Parrinello-Rahman (1 bar) respectively. Again, PBC and PME schemes were applied.

Results and discussion

Docking studies

Molecular docking study was carried out not just to investigate the amino acid residues for binding the ligand, but also to predict the orientation of our ligands in the *Aa*EST2 active site.

The first step for the dissociative paroxon reaction that inhibits the *Aa*EST2 is the interaction between Ser155 and the phosphorous site of the ligand.[6] Thus, our first criteria to choose the best representative pose was to take into account this key structural information. In other words, the first sieve of our docking results was to consider just poses with short distances between the phosphorous site of the ligands and Ser155 allowing their interaction along the MD. Then, the pose with the best score was chosen for each ligand. Table 1 resumes the interaction energies, affinities, H-bonds energies and protein H-bond residues of each chosen pose.

Table 1: Interaction energies, affinities and H-bonds of the studied pesticides.

	Interaction (kJ/mol)	**Affinity (kJ/mol)**	**H-bond (kJ/mol)**	**H-bond interaction residues**
Chlorpyrifos	-108.29	-39.34	-4.90	Ser155, Ser185

Diazinon	-103.92	-29.23	-6.03	Ser155, Ser185
Parathion	-94.23	-27.73	-8.83	Ser155, Ser185
Paraoxon	-97.71	-26.37	-7.22	Ser155

Figure 3 depictures the active site of *Aα*EST2 with the chosen ligand pose docked in. It is interesting to note that, as a result of the docking analyses, all the ligands have their aromatic ring sufficiently close to the residue Trp85 allowing their interaction and, consequently, their energy exchange in a dynamic picture. The frames in Figure 3 were considered the starting points of our molecular dynamics simulations.

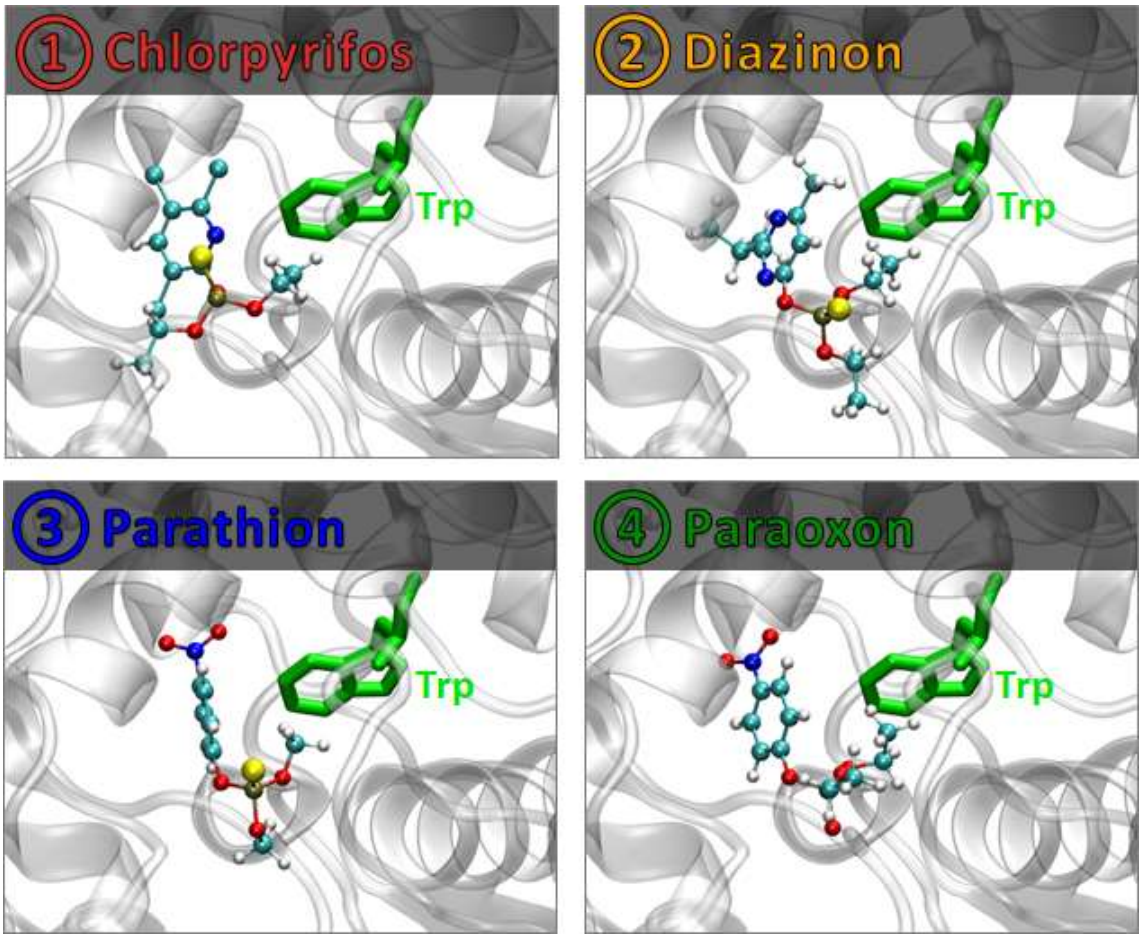

Figure 3: Molecular dynamics starting points. Residue Trp85 is highlight in green.

MD simulations

To monitor the evolution of the MD simulations, in Figure 4 we report the RMSD (root-mean-square deviation) analyses for the four systems conducted on heavy atoms of the protein backbone and on heavy atoms of the ligands. The plots show the RMSD after the discard of the first 20 ns of simulation.

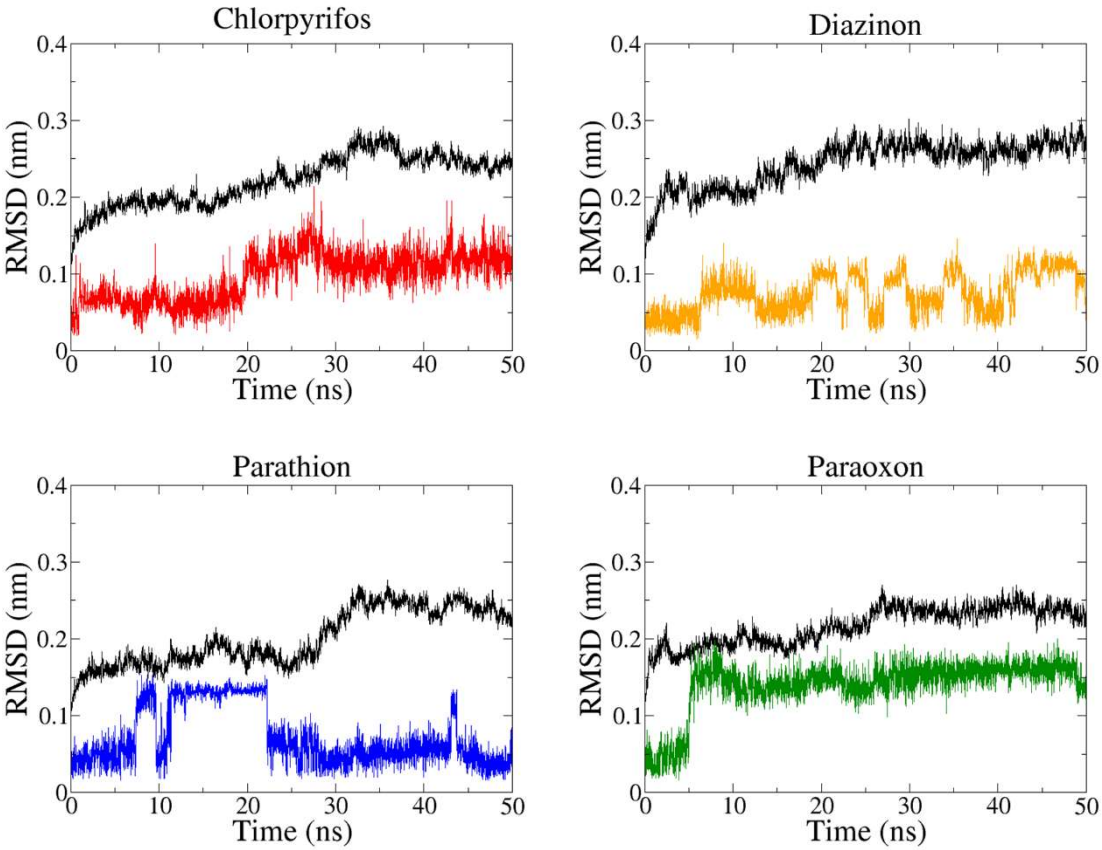

Figure 4: RMSD plots of the protein (black curve) and the ligands after discard the first 20 ns.

The protein backbone in all systems is reasonable equilibrated after 20 ns of simulation. The profiles of the graphs, the amount of the data and the long simulated time confirm that we were able to properly sample the fluctuations around the crystallographic minimum.

Because of the conjugated nature of the pesticides and Trp85 in the active site of *Aa*EST2, we decided to investigate the hypothesis that the studied pesticides are able to remove energy from the cited residue through a quenching process. Clearly, because of the electronic nature of the processes involved in energy transfer, we cannot directly evaluate them from classic MD. However, Förster theory can be employed for a first understanding. As we discussed in the theoretical section, the coupling between the donor and the acceptor (in our hypothesis the Trp85 would be the donor and the

pesticide the acceptor) is dependent on the centre of mass distance and its orientation, which are classic parameters and can be taken from the MD simulations.

For our analyses, we considered the same time window shown in RMSD plots i.e., we discarded the first 20 ns of MD simulation in order to guarantee that the systems were equilibrated. Hence, the last 50 ns were analysed through a new methodology based in Förster theory[25] that consists in center enlarged van der Waals spheres on the conjugated rings of the pesticides and in Trp85. In sequence, we were able to compute the interlocked volumes of the spheres as illustrated in Figure 5.

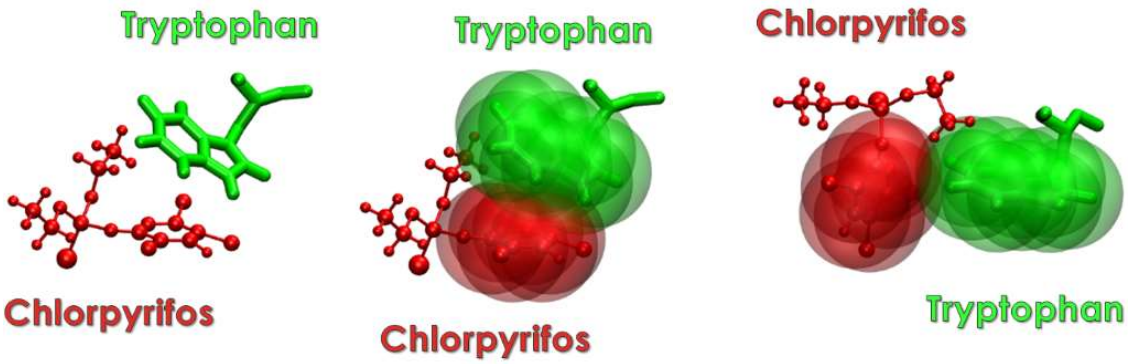

Figure 5: Interlocked spheres volumes examples

By applying Förster theory, we can interpret our results in the following way: the greater is the superimposed volume, the closer and more favourably well-oriented donor and acceptors will be. Thus, we can use the superimposition volume as a prelaminar study to have a clue about the probability of energy exchange.

Analysing the 5000 frames of the trajectory using this new model, we found the result presented in Figure 6.

Figure 6: Computed interlocked volumes between OPs and TRp85 during 50 ns of MD simulation.

Figure 6 indicates that we may have a higher interaction between Trp85 and the pesticides in this order: chlorpyrifos, diazinon, parathion and paraoxon. This result shows that, because of its orientation along the molecular dynamics, chlorpyrifos may quench Trp85 in a more efficient way comparing to the others pesticides analysed. Thus, we expect that, in the presence of those pesticides, *Aa*EST2 (that is intrinsically fluorescent) will present a lower fluorescent intensity than the *Aa*EST2 pure.

The experimental results obtained by Carullo *et al*[6], and reported here in Figure 7, show that the fluorescence signal of the system containing chlorpyrifos is lower in intensity than the ones of the systems containing diazinon and parathion, for concentrations ranging from 0.2 to 1.0 nmolar. This result corroborate our hypothesis that this reduction in fluorescence could be related to the interactions with Trp85 and explained by FRET.

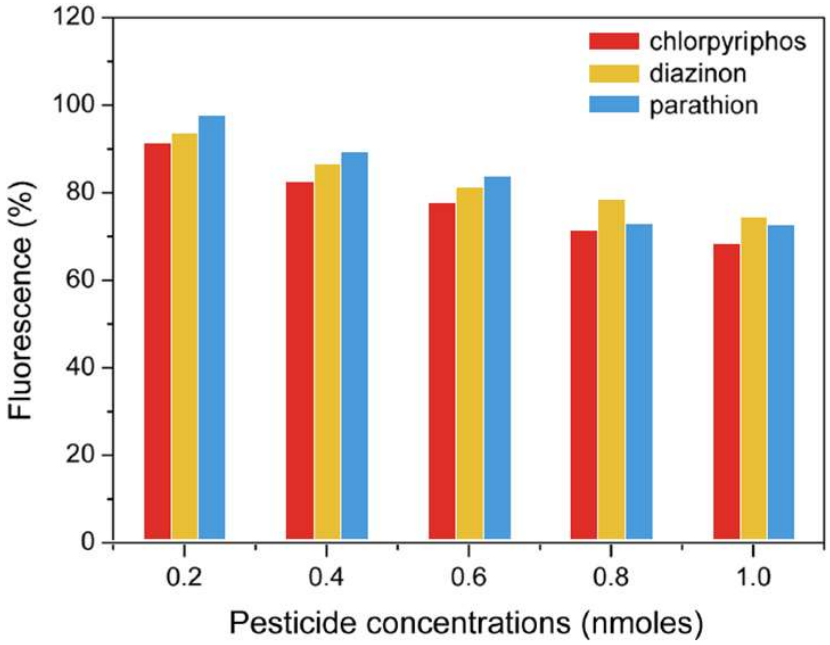

Figure 7: Experimental results of OP fluorescence reported by Carullo et al[6]

Conclusions

From the obtained experimental results, we confirm our initial hypothesis that pesticides are able to quench the Trp85 of *Aa*EST2. From our studies we may conclude that chlorpyrifos is, among the analysed pesticides, the molecule that most interacts with the Trp85, due to the proximity and orientation between them. On the other hand, paraoxon is, apparently, the molecule that has the lower interaction with Trp85, and consequently, in its presence, *Aa*EST2 would present the highest fluorescence signal and a lower quench.

Acknowledgments

The authors wish to thank the Military Institute of Engineering, University of Hradec Kralové and University of Defense for the infrastructure, the Brazilian financial agencies CNPq (Grants nº 306156/2015-6 and 155821/2016-4), FAPERJ (Grant no E-

02/202.961/2017), for financial support and MoLECoLab colleagues for the discussions. This work was also supported by the excellence project FIM.

References

1. Perezgasga, L., Sánchez-sánchez, L., Aguila, S. & Vazquez-duhalt, R. Substitution of the Catalytic Metal and Protein PEGylation Enhances Activity and Stability of Bacterial Phosphotriesterase. *Appl Biochem Biotechnol* **166,** 1236–1247 (2012).

2. Castro, A. A. De, Prandi, I. G., Kuca, K. & Ramalho, T. C. Organophosphorus degrading enzymes: Molecular basis and perspectives for enzymatic bioremediation of agrochemicals. **41,** 471–482 (2017).

3. Quinn, D. M. Acetylcholinesterase: Enzyme Structure, Reaction Dynamics, and Virtual Transition States. *Chem. Rev.* **87,** 955–979 (1987).

4. Organisation for the prohibition of chemical weapons. Available at: https://www.opcw.org/. (Accessed: 16th October 2017)

5. Colovic, M. B., Krstic, D. Z., Lazarevic-Pasti, T. D., Bondzic, A. M. & Vasic, V. M. Acetylcholinesterase Inhibitors: Pharmacology and Toxicology. *Curr. Neuropharmacol.* **11,** 315–335 (2013).

6. Carullo, P., Cetrangolo, G. P., Mandrich, L., Manco, G. & Febbraio, F. Fluorescence Spectroscopy Approaches for the Development of a Real-Time Organophosphate Detection System Using an Enzymatic Sensor. *Sensors* 3932–3951 (2015). doi:10.3390/s150203932

7. De Simone, G. *et al.* The crystal structure of a hyper-thermophilic carboxylesterase from the archaeon Archaeoglobus fulgidus. *J. Mol. Biol.* **314,** 507–518 (2001).

8. Forster, T. Energiewanderung und Fluoreszenz. *Naturwissenschaften* **33,** 166–175 (1946).

9. Ghisaidoobe, A. B. T. & Chung, S. J. Intrinsic Tryptophan Fluorescence in the

Detection and Analysis of Proteins : A Focus on Förster Resonance Energy Transfer Techniques. 22518–22538 (2014). doi:10.3390/ijms151222518

10. Pinheiro, S. & Curutchet, C. Can Förster Theory Describe Stereoselective Energy Transfer Dynamics in a Protein − Ligand Complex ? *J. Phys. Chem. B* **121,** 2265–2278 (2017).

11. TEALE, F. W. J. & WEBER, G. Ultraviolet Fluorescence of the Aromatic Amino Acids. **65,** 476–482 (1954).

12. Hehre, W. J. & Deppmeier, B. J. *PC SPARTAN Pro. Wavefunction, Inc., Irvine, 1999*. (Wavefunction, 1999).

13. Berman, H. M. *et al.* The Protein Data Bank. *Nucleic Acids Res.* **28,** 235–242 (2000).

14. Thomsen, R. & Christensen, M. H. MolDock: a new technique for high accuracy molecular docking. *J. Med. Chem.* **49,** 3315–3321 (2006).

15. Van Der Spoel, D. *et al.* GROMACS: Fast, flexible, and free. *J. Comput. Chem.* **26,** 1701–1718 (2005).

16. Toukan, K. & Rahman, A. Molecular-dynamics study of atomic motions in water. *Phys. Rev. B* **31,** 2643–2648 (1985).

17. Schuler, L. D., Daura, X. & Van Gunsteren, W. F. An improved GROMOS96 force field for aliphatic hydrocarbons in the condensed phase. *J. Comput. Chem.* **22,** 1205–1218 (2001).

18. Chiu, S., Pandit, S. A., Scott, H. L. & Jakobsson, E. An Improved United Atom Force Field for Simulation of Mixed Lipid Bilayers. *J. Phys. Chem. B* **113,** 2748–2763 (2009).

19. Malde, A. K. *et al.* An Automated force field Topology Builder (ATB) and repository: Version 1.0. *J. Chem. Theory Comput.* **7,** 4026–4037 (2011).

20. Abraham, M. J. *et al. GROMACS User Manual v. 5.1*. (2015).

21. Berendsen, H. J. C., Postma, J. P. M., van Gunsteren, W. F., DiNola, a & Haak, J. R. Molecular dynamics with coupling to an external bath. *J. Chem. Phys.* **81,** 3684–

3690 (1984).

22. Bussi, G., Donadio, D. & Parrinello, M. Canonical sampling through velocity rescaling. *J. Chem. Phys.* **126,** (2007).

23. Darden, T., York, D. & Pedersen, L. Particle mesh Ewald: An N·log(N) method for Ewald sums in large systems. *J. Chem. Phys.* **98,** 10089–10092 (1993).

24. Hess, B., Bekker, H., Berendsen, H. J. C. & Fraaije, J. G. E. M. LINCS: A linear constraint solver for molecular simulations. *J. Comput. Chem.* **18,** 1463–1472 (1997).

25. Cupellini, L., Jurinovich, S., Prandi, I. G., Caprasecca, S. & Mennucci, B. Photoprotection and triplet energy transfer in higher plants: The role of electronic and nuclear fluctuations. *Phys. Chem. Chem. Phys.* **18,** 11288–11296 (2016).